Optical properties of the filled tetrahedral semiconductors LiMgX (X = N, P and As)

2006 J. Phys.: Condens. Matter 18 7237

(http://iopscience.iop.org/0953-8984/18/31/018)

INSTITUTE OF PHYSICS PUBLISHING JOURNAL OF PHYSICS: CONDENSED MATTER

J. Phys.: Condens. Matter **18** (2006) 7237–7247 doi:10.1088/0953-8984/18/31/018

Optical properties of the filled tetrahedral semiconductors LiMgX (X = N, P and As)

F Kalarasse, B Bennecer[1] and A Mellouki

Physics Laboratory at Guelma, Faculty of Science and Engineering, University of Guelma, PO Box 401 Guelma 24000, Algeria

E-mail: b_bennacer@hotmail.com

Received 11 May 2006, in final form 27 June 2006
Published 21 July 2006
Online at stacks.iop.org/JPhysCM/18/7237

Abstract

First principles calculations, by means of the full-potential linearized augmented plane wave method within the local density approximation, were carried out for the electronic and optical properties of the filled tetrahedral compounds LiMgN, LiMgP and LiMgAs. The bandgap trend in the ternaries is found to be similar to the one encountered in the zinc-blende AlX. The assignment of the structures in the optical spectra and band structure transitions are investigated in detail. The predicted values of the dielectric constants for LiMgN, LiMgP and LiMgAs are close to those of the binary compounds AlN, AlP and AlAs.

(Some figures in this article are in colour only in the electronic version)

1. Introduction

The filled tetrahedral semiconductors LiMgX (X = N, P, As) form a special class of the Nowotny–Juza $A^{I}B^{II}C^{V}$ compounds [1–8]. Their wide bandgap makes them very prominent materials for technological applications. Thus, several studies have been carried out in order to investigate their properties. Theoretically, the electronic structure has been reported by Li *et al* [9] and Yu *et al* for LiMgN [10] and Yu *et al* for LiMgP [11]. Recently, the bandgaps and the nature of bonding in LiMgX compounds have been examined by Kandpal *et al* [12], and the structural and elastic properties have been calculated by two of us [13]. Experimentally, Kuriyama and his team have measured the bandgaps of these compounds [4, 6, 7] and they have reported photoluminescence and Raman scattering studies for LiMgP [5, 8]. Furthermore, they have shown that the substitution of Zn atom in LiZnX compounds by the lighter atom Mg widens their gaps.

[1] Author to whom any correspondence should be addressed.

Despite these reported results and besides the measurement of the absorption coefficient in a narrow region around the absorption edge for LiMgP [4] and LiMgAs [6], there is still a lack of information about their physical properties in general and optical properties in particular.

In this paper, we present first principles studies of the electronic and the linear optical properties of α-LiMgX compounds. The calculations are performed using the full potential linear augmented plane wave (FP–LAPW) method [14, 15], in conjunction with the local density approximation (LDA) [16]; the features of the obtained optical spectra are assigned to interband transitions along the high symmetry lines in the Brillouin zone (BZ). The static dielectric constants are also calculated and compared to those of the binary zinc-blende analogous AlX compounds. The rest of this paper is organized as follows; in section 2 we describe the method and we give details of the calculations; in section 3 the obtained results are given and discussed. A conclusion is given in section 4.

2. Computational details

The present calculations are performed using the full potential linear augmented plane wave method within the local density approximation (LDA), as implemented in the Wien2k code [15]. In this method the space is divided into non-overlapping muffin-tin (MT) spheres separated by an interstitial region, in this context the basis functions are expanded in combinations of spherical harmonic functions inside the muffin-tin spheres and plane waves in the interstitial region. In this work we treat the core electrons fully relativistically, and the valence electron scalar relativistically (all the relativistic effect are taken into account except the spin–orbit coupling).

In the calculations, the Li ($2s^1$), Mg ($3s^2$), N ($2s^22p^3$), P ($3s^23p^3$), As ($3d^{10}4s^24p^3$) and Al ($3s^23p^1$) states are treated as valence electrons, and the muffin-tin radii are chosen to be 1.9 for all atoms in LiMgN and 2.2 in LiMgP and LiMgAs. The basis functions are expanded up to $R_{\mathrm{mt}} \times K_{\mathrm{max}} = 8$ (where K_{max} is the plane wave cut-off and R_{mt} the smallest of all MT sphere radii), and up to $l_{\mathrm{max}} = 10$ in the expansion of the non-spherical charge and potential. We use the Perdew and Wang functional [16] for the exchange and correlation interaction. For the integration we used $7 \times 7 \times 7$ k-points mesh in the whole first Brillouin zone and the self-consistent calculations are considered to be converged when the total energy is stable within 0.1 mRyd.

The linear optical properties in solids can be described with the complex dielectric function $\varepsilon(\omega) = \varepsilon_1(\omega) + \mathrm{i}\varepsilon_2(\omega)$, the interband contribution to the imaginary part of $\varepsilon(\omega)$ is calculated by summing transitions from occupied to unoccupied states over the Brillouin zone, weighted with the appropriate momentum matrix elements. In the present calculations the imaginary, or absorptive part of the dielectric tensor, is given by [17]

$$\mathrm{Im}\,\varepsilon(\omega) = \varepsilon_2(\omega) = \frac{4\pi^2 e^2}{m^2\omega^2} \sum_{i,j} \int |\langle i|M|j\rangle|^2 (f_i(1-f_j))\delta(E_f - E_i - \hbar\omega)\,\mathrm{d}^3k \qquad (1)$$

where e and m are the electron charge and mass, respectively, ω is the frequency of the photon, M is the momentum operator, $|i\rangle$ is the wavefunction, corresponding to eigenvalue E_i, and f_i is the Fermi distribution for $|i\rangle$ state. The integral over the Brillouin zone (BZ) was performed using the tetrahedron method. The calculated optical spectra depend strongly on the BZ sampling, therefore a sufficiently dense k-mesh is used in the calculations of optical spectra, which consists of $25 \times 25 \times 25$ k-mesh.

Table 1. Structural parameter, lattice parameter a_0 in (Å), Bulk modulus B in (GPa), bulk modulus pressure derivative B' of α-LiMgX and their binary analogous zinc-blende AlX.

	Filled compound			Binary analogous		
	This work	Other	Expt.	This work	Other	Expt.
	LiMgN			AlN		
a_0	4.91	5.009[a], 5.072[b], 4.593[c]	4.955[d]	4.35	4.32[e], 4.334[f], 4.342[g], 4.353[h]	4.38[h]
B	112.99	97.66[a], 80.1[b], 147.2[c]		214.7	203[e], 216[f], 207[g]	
B'	4	3.99[a]		4.09	3.2[e], 4.0[f]	
	LiMgP			AlP		
a_0	5.91	6.01[i], 6.028[b]	6.005[j]	5.44	5.508[i]	5.46[k]
B	59.31	52.9[i], 49.6[b]		90.0	81.52[i]	95[k]
B'	3.93	3.88[i]		4.1	3.89[i]	
	LiMgAs			AlAs		
a_0	6.08	6.218[b]	6.181[l]	5.64		5.66[k]
B	51.57	42.9[b]		75.0		78[k]
B'	4.12			4.7		

[a] Reference [10]. [b] Reference [12]. [c] Reference [9]. [d] Reference [7]. [e] Reference [19]. [f] Reference [20]. [g] Reference [21]. [h] Reference [22]. [i] Reference [11]. [j] Reference [4]. [k] Reference [23]. [l] Reference [5].

Table 2. Calculated and experimental bandgaps (eV) for LiMgN, LiMgP and LiMgAs.

	Direct gap (Γ–Γ)		Indirect gap (Γ–X)		
	This work	Other	This work	Other	Expt
LiMgN	2.82	2.51 [10]	2.46	2.47 [10]	3.2 [7]
LiMgP	2.54	2.41 [11]	1.38	1.55 [11]	2.43 [4]
LiMgAs	1.78		1.25		2.29–2.38 [6]

3. Results and discussion

3.1. Structural and electronic properties

The equilibrium structural parameters are determined by fitting the total energy as a function of volume to the Murnaghan's equation of state (eos) [18]. The obtained results for the α and β phases together with the elastic properties for the former have been reported elsewhere [13]. The structural parameters of the most stable α phase are listed in table 1, in which the available experimental data and results of other calculations are also shown. The lattice parameters and the bulk moduli agree well with the other calculations. The electronic band structures, density of states and optical spectra are calculated at the theoretical lattice constants.

The calculated band structures and the corresponding total density of states (DOS) are shown in figure 1 for the three studied compounds.

The first peak encountered in the DOS, if we start from lower energies, consists entirely of the group V (i.e., N, P and As) s states. This peak is centred around −12, −10 and −10 eV for LiMgN, LiMgP and LiMgAs, respectively (see figures 2–4) where the site and angular momentum decomposed DOS are shown. Its width originates from the region around the Γ point in the Brillouin zone in the low lying band in figure 1. The next structure consists mainly of group V atom p states and there is also a small contribution from the metal atom p ones. Continuing upward in energy, it is clear from figure 1 that all the studied compounds are semiconductors. The conduction bands are mixture of s and p states and for the low lying ones (below 5 eV) the contribution of the Li s states is very low in LiMgN than in LiMgP and LiMgAs.

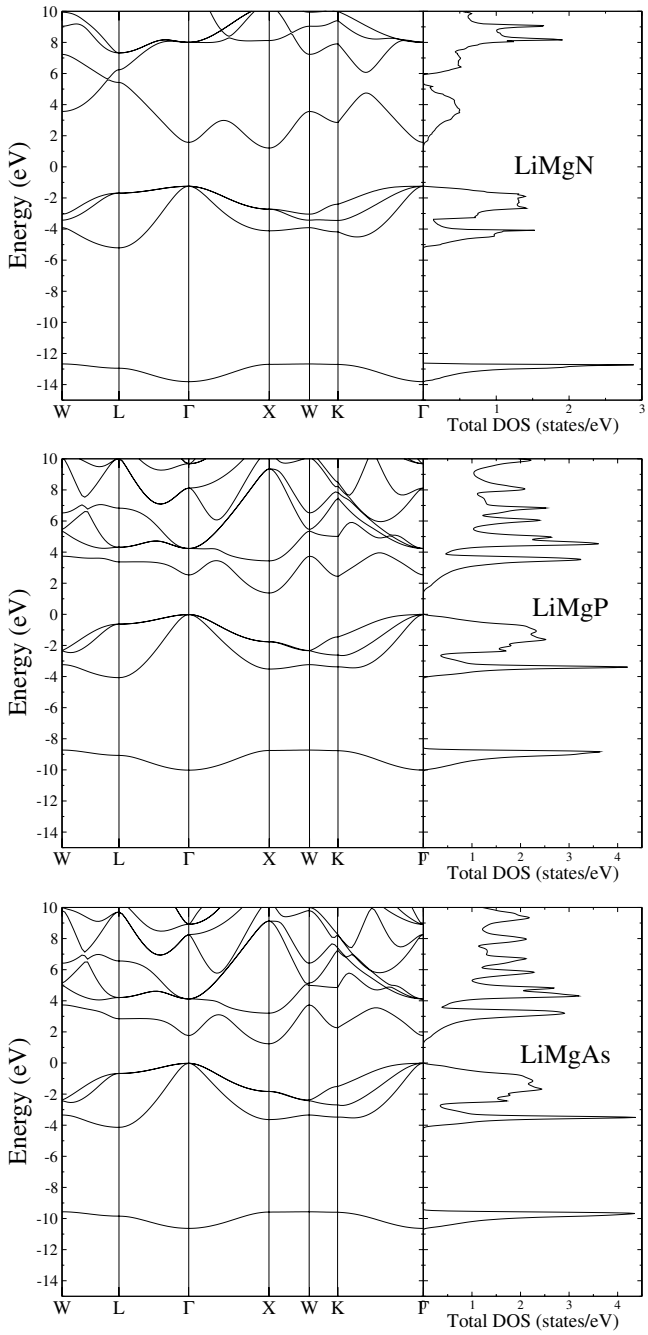

Figure 1. Electronic band structure (left panels) and total density of states (right panels) for the ternary compounds LiMgN, LiMgP and LiMgAs, the Fermi level is set to zero.

The calculated bandgaps are listed in table 2 together with the results of other calculations and the experimental values. As seen in this table the studied compounds have indirect gaps, consistent in nature with those reported by Li *et al* [9] and Yu *et al* [10] for LiMgN and by

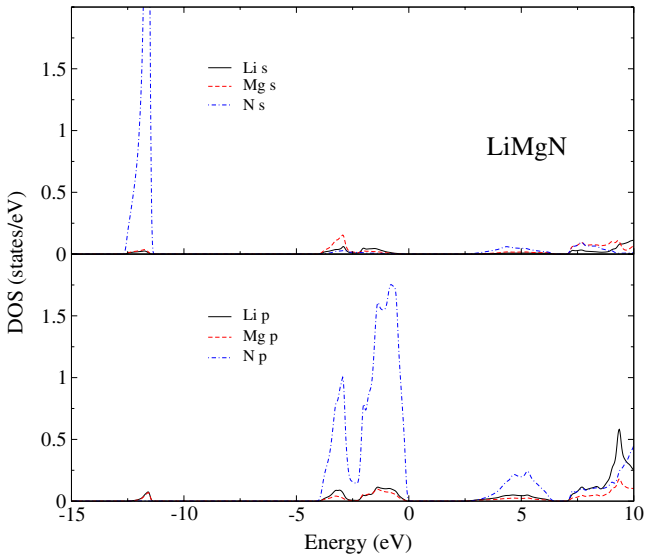

Figure 2. Site and angular momentum decomposed DOS of LiMgN, the Fermi level is set to zero.

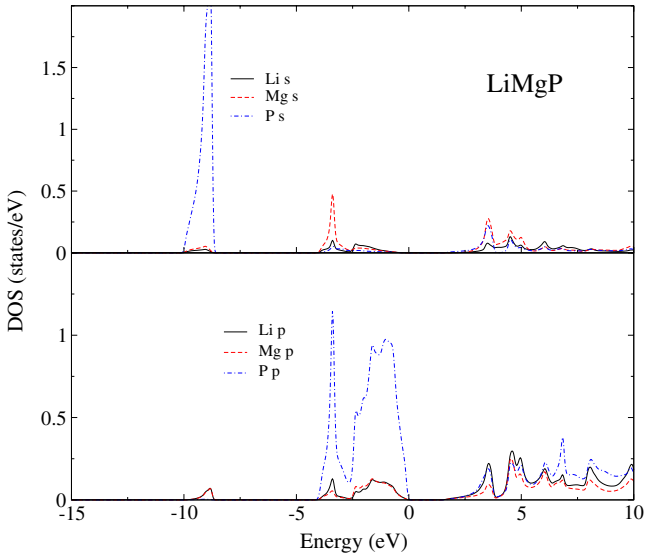

Figure 3. As figure 2, but for LiMgP.

Yu *et al* [11] for LiMgP, but the experimental ones are direct. For LiMgN, our calculated gap values are close the those given in [10] but smaller than the ones reported in [9], which were obtained using *ab initio* pseudopotential method with a lattice parameter (4.593 Å) smaller than the equilibrium one (4.91 Å) used in this study. The LiMgX compound gaps have the same trend as the one born by experimental measurements and the one encountered in the analogous binaries AlX; i.e., they decrease in this sequence LiMgN–LiMgP–LiMgAs. The discrepancy between theoretical and experimental gaps is attributed to the LDA which always underestimates the bandgap. It is worth noting that the gaps for LiMgX are larger than those for LiZnX compounds [24].

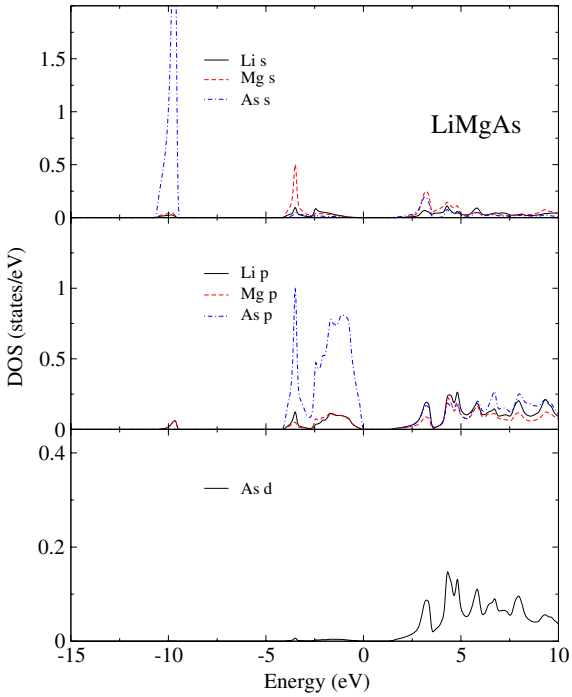

Figure 4. As figure 2, but for LiMgAs.

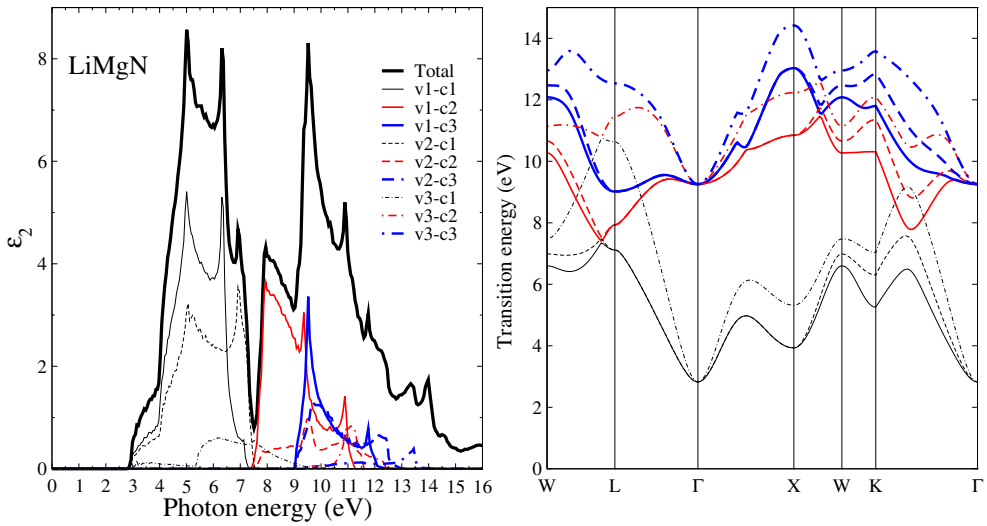

Figure 5. The decomposition of the imaginary part of the dielectric function into band-to-band contributions (left panel) and the transition energy band structure (right panel) for LiMgN. The counting of the bands is down (up) from the top (bottom) of the valence (conduction) band.

3.2. Optical properties

The absorptive (imaginary) parts of the dielectric function ε_2, are displayed in figures 5–7 for the studied compounds. The spectrum of LiMgN is different from the others. The analysis of

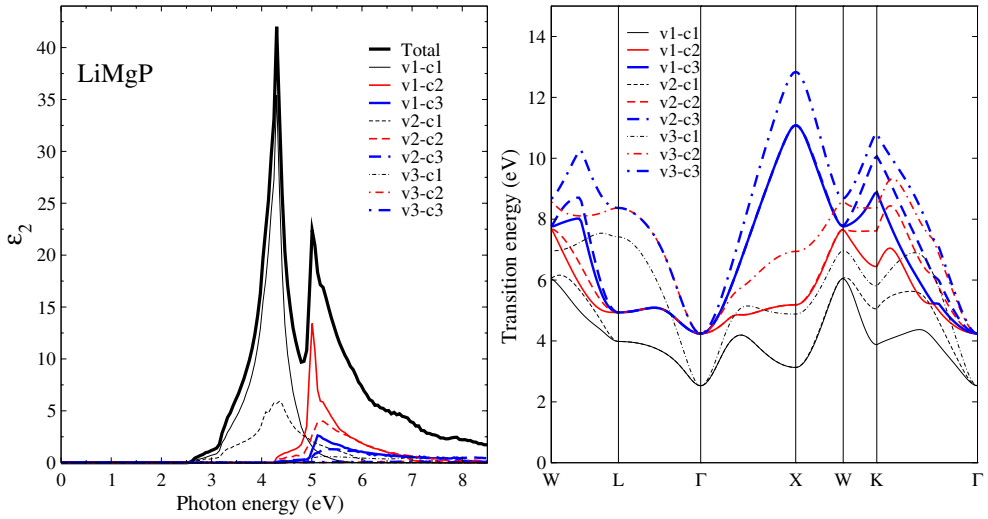

Figure 6. As figure 5, but for LiMgP.

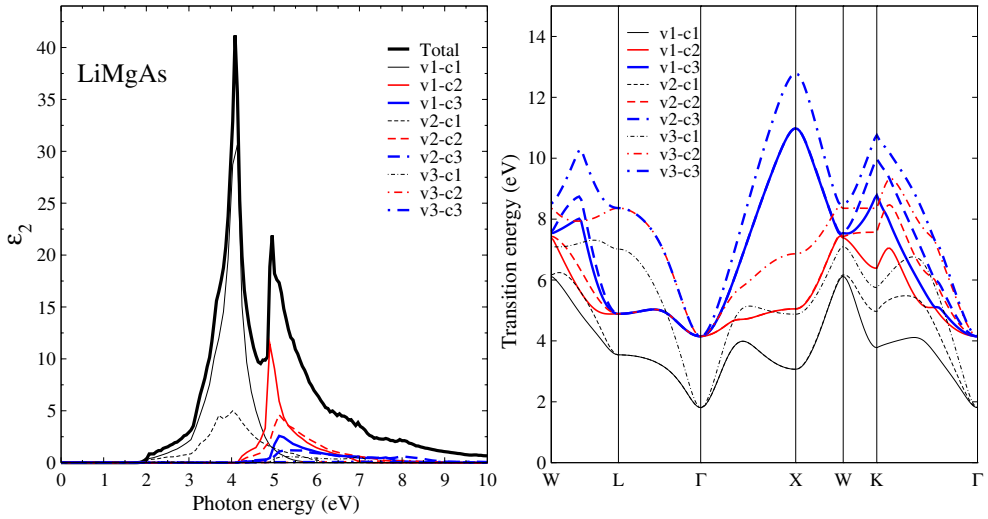

Figure 7. As figure 5, but for LiMgAs.

the calculated optical spectra and the determination of the origins of the different peaks and features are performed on the basis of decomposing each spectrum to its individual pair contribution, i.e. the contribution from each pair of valence vi and conduction cj bands (vi–cj), and plotting the transition (from valence to conduction) band structures, i.e. the transition energy $(k) = E_{cj}(k) - E_{vi}(k)$ (see figure 5). These techniques allow knowledge of the bands which contribute more to the peaks and their locations in the Brillouin zone [20, 25–27]. The positions of the peaks and the corresponding interband transition and their locations in the Brillouin zone are reported in tables 3–5 for the three studied compounds. To the best of the author's knowledge no experimental spectra are available for these compounds. The details of the optical spectra are given below.

Table 3. Optical transitions in α-LiMgN.

Energy of optical structure Peak position (eV)	Major contribution transitions	
	Transition	Energy (eV)
3.93	X, Δ:v1, v2 $\rightarrow$ c1	3.92
4.97	Λ, Δ, Σ: v1; v2 $\rightarrow$ c1	4.95; 4.98
6.30	X–W–K, Λ, Σ: v1 $\rightarrow$ c1	6.31, 6.35
	K, Λ, Σ: v2 $\rightarrow$ c1	6.30
	X–W, Λ, Σ: v3 $\rightarrow$ c1	6.31, 6.35
6.92	Near W, Λ, Σ: v2 $\rightarrow$ c1	6.92
	X–W, Λ, Σ: v3 $\rightarrow$ c1	6.92
7.16	Q, Λ, Σ: v1 $\rightarrow$ c1	7.16
7.52	Q: v1 $\rightarrow$ c2	7.52
7.82	Q, Σ: v1 $\rightarrow$ c2	7.82
7.93	Q, Σ: v1 $\rightarrow$ c2	7.94
	Q, L: v2 $\rightarrow$ c2	7.90
9.35	Δ, Λ, Σ: v1 $\rightarrow$ c2	9.33
9.48	Δ, Λ, Σ: v1 $\rightarrow$ c3, v2 $\rightarrow$ c2	9.43, 9.48
	Δ, Λ, Σ: v2 $\rightarrow$ c3	9.59
10.82	Δ: v1 $\rightarrow$ c2	10.82
	Near X (X–W): v2 $\rightarrow$ c2	10.82
11.66	Q, W–K, Δ, Σ: v1 $\rightarrow$ c3	11.67
11.90	Q, Δ, X–W, Σ: v2 $\rightarrow$ c3	11.90
13.37	Q, X–W–K, Σ: v3 $\rightarrow$ c3	13.37

Table 4. Optical transitions in α-LiMgP.

Energy of optical structure Peak position (eV)	Major contribution transitions	
	Transition	Energy (eV)
3.25	Λ, Δ, X–W, Σ: v1, v2 $\rightarrow$ c1	3.25
4.34	Q, X–W, Σ: v1 $\rightarrow$ c1	4.33
	Q, X–W, Σ: v2 $\rightarrow$ c1	4.09, 4.30, 4.38
4.88	Λ, Δ, Σ: v1 $\rightarrow$ c2	4.88
4.99	Q, Λ, Δ, Σ: v1 $\rightarrow$ c2	4.99
5.05	Q, Δ, Σ: v1 $\rightarrow$ c3	5.10
	Q, Δ, Σ: v2 $\rightarrow$ c2	5.11
5.24	Λ, Δ, Σ: v3 $\rightarrow$ c1	5.22
	Q, Δ, Σ: v2 $\rightarrow$ c3	5.34

LiMgN. The spectrum of LiMgN is quite different from the two others; it is too broad and contains more structure than those of LiMgP and LiMgAs. The threshold in ε_2 occurs at 2.82 eV and this corresponds to the direct gap at Γ. Besides the shoulder in 3–4 eV region which originates from the transitions from the three highest valence bands to the first conduction band in ΓL, ΓX and ΓK directions, the spectrum can be divided into three groups of structures. The first structure in the energy range 4.5–7.5 eV, as is clear from figure 5, is mainly due to the interband transitions from the two highest valence bands to the lowest conduction band with a small contribution from the third valence band to the first conduction one. The three peaks in this structure, in increasing energy, arise from the Γ–X direction, the Γ–K direction and the vicinity of the W point, respectively (see table 3). The second group (7.5–10 eV) originates mainly from the highest valence to the second and third conduction band transitions in the

Table 5. Optical transitions in α-LiMgAs.

Energy of optical structure Peak position (eV)	Major contribution transitions	
	Transition	Energy (eV)
3.07	Δ: v1 $\rightarrow$ c1	3.07
3.21	Δ: v2 $\rightarrow$ c1	3.21
3.63	Q, Δ: v1, v2 $\rightarrow$ c1	3.63
4.08	Q, Δ, Σ: v1 $\rightarrow$ c1	3.98
	Q, Σ: v2 $\rightarrow$ c1	4.01, 4.08
4.75	Δ, Σ: v1, v2 $\rightarrow$ c2	4.75, 4.76
4.91	L, Δ, Σ: v1 $\rightarrow$ c2	4.88, 4.91
5.05	Q, Δ, Σ: v1 $\rightarrow$ c3	5.03
	Λ, Δ, Σ: v1 $\rightarrow$ c2	5.04
	Q, X–W, Σ: v2 $\rightarrow$ c2	5.09

Table 6. The calculated dielectric constants of α-LiMgX and their binary analogues AlX, together with the available experimental and other calculation results. ΔE is the energy shift.

Materials	Uncorrected	Corrected	Other	Expt	ΔE (eV)
LiMgN	4.91	4.66			0.43
AlN	4.55	4.31	3.90 [20] 5.24 (4.46) [22][a]	4.68 [20][b]	0.59
LiMgP	7.77				
AlP	9.00	8.30	8.16 [29][c]	8.0 [29][c]	0.45
LiMgAs	8.55	7.74			0.51
AlAs	10.05	8.11	8.83 [29][c]	8.16 [29][c]	1.16

[a] Reference [22] value in parentheses is the corrected one.
[b] Wurtzite structure.
[c] See [29] and references therein.

neighbourhood of L and Γ points in the BZ. The third group of structures corresponding to the photon energy greater than 10 eV is due to the transitions from the three highest valence bands to the second and third conduction ones.

LiMgP and LiMgAs. The imaginary parts of the dielectric function of LiMgP and LiMgAs are quite similar (see figures 6 and 7). The positions of the peaks and the major contributions are listed in tables 4 and 5. The most striking feature in these spectra is the absence of the first peak (E_1) in comparison to the other filled tetrahedral compounds LiZnP and LiZnAs [24]. In the latter the E_1 peak arises from transitions occurring around the L point, while the E_2 peak arises from transitions in the Δ line and around the X point. The absence of the E_1 peak in LiMgP and LiMgAs may be attributed to the fact that the energy gaps around L and K points and on the Δ line are very close (see figures 6 and 7); so, the position of the E_1 peak overlaps with the slope of its E_2 peak. We point out that the difference between the gaps is larger in LiMgAs (a hip at 3.63 eV) than it is in LiMgP.

The main peak (E_2) occurs at 4.34 and 4.08 eV for LiMgP and LiMgAs, respectively, and originates from the transitions from the highest valence to the first conduction band in the Δ and Σ lines. The position of this peak is shifted to lower energies compared to the calculated one for the binary compounds AlP and AlAs by Huang and Ching [28], while conserving the same trend.

The third peak (E_1') arises mainly from the two highest valence to second conduction band transitions in L–Γ, Γ–X and Γ–K directions. There is also a small contribution from the transitions from the highest valence to the third conduction bands in the Σ, Δ and Q lines.

Like the fundamental gap, the static dielectric constant $\varepsilon(0)$ is a very important physical quantity for semiconductors. The LDA calculations generally tend to overestimate its value [29, 30], depending on the degree of underestimation of the gap. This overestimation is corrected by allowing a constant energy shift for the conduction bands of 0.43 and 0.51 eV for LiMgN and LiMgAs, respectively. For LiMgP our calculated direct energy gap is greater than the measured one. The obtained theoretical values of $\varepsilon(0)$ (with and without shift) are reported in table 6. For AlP and AlAs, the corrected values of $\varepsilon(0)$ are in good agreement with the experimental ones. For AlN our calculated value (4.66) is very close to the one reported by da Silva *et al* [22] (4.46). This might be a measure of the reliability of the predicted values for the ternaries.

4. Conclusion

In conclusion, we have presented a first principles study of the optical spectra of the three filled tetrahedral compounds LiMgN, LiMgP and LiMgAs. In our calculations the FP–LAPW in the LDA scheme has been used. The calculated optical spectra are quite similar for LiMgP and LiMgAs. The decomposition of the dielectric functions into individual band-to-band contributions and the transition band structures allowed us to identify the microscopic origin of the features in the optical spectra and the contributions of the different regions in the Brillouin zone. The calculated static dielectric constants of the ternaries obtained by correcting the calculated bandgaps, with the scissor operator, predict that they are close to the those of the binaries AlN, AlP and AlAs.

Acknowledgments

One of the authors (B Bennecer) is very grateful to Professor P Blaha and his team (Vienna University of Technology, Austria) for providing the wien2k package used in performing this calculation.

References

[1] Nowotny H and Bachmayer K 1949 *Mh. Chem.* **80** 734
[2] Juza R and Hund F 1948 *Z. Anorg. Chem.* **257** 1
[3] Juza R, Langer K and Benda K V 1968 *Angew. Chem. Int. Edn* **7** 360
[4] Kuriyama K, Kushida K and Taguchi R 1998 *Solid State Commun.* **108** 429
[5] Kuriyama K and Kushida K 2000 *J. Appl. Phys.* **87** 2303
[6] Kuriyama K and Kushida K 2000 *J. Appl. Phys.* **87** 3168
[7] Kuriyama K, Nagasawa K and Kushida K 2002 *J. Cryst. Growth* **237–239** 2019
[8] Kuriyama K and Kushida K 1999 *Solid State Commun.* **112** 429
[9] Li H-P, Hou Z-F, Huang M-C and Zhu Z-Z 2003 *Chin. Phys. Lett.* **20** 114
[10] Yu L H, Yao K L and Liu Z L 2004 *Physica* B **353** 278
[11] Yu L H, Yao K L and Liu Z L 2005 *Solid State Commun.* **135** 124
[12] Kandpal H C, Felser C and Seshadri R 2006 *J. Phys. D: Appl. Phys.* **39** 776
[13] Bennecer B and Kalarasse F 2006 *CISGM-4: Proc. 4th Int. Congress on Material Science and Engineering (Tlemcen, Algeria, May, 2006)*; *Algerian J. Adv. Mater.* **3** 23–6 (ISSN: 1111-625X)
[14] Singh D 1994 *Planes Waves, Pseudo-Potentials and the LAPW Method* (Dortrecht: Kluwer Academic)
[15] Blaha P, Schwarz K, Madsen G K H, Kvasnicka D and Luitz J 2001 *WIEN2k, An Augmented Plane Wave + Local Orbitals Program for Calculating Crystal Properties* (Austria: Karlheinz Schwarz, Techn. Universität Wien) ISBN 3-9501031-1-2
[16] Perdew J P and Wang Y 1992 *Phys. Rev.* B **45** 13244
[17] Ambrosch-Draxl C and Sofo J O 2004 Linear optical properties of solids within the full-potential linearized augmented plane wave method *Preprint* cond–mat/0402523

[18] Murnaghan F D 1944 *Proc. Natl Acad. Sci. USA* **30** 244
[19] Kim K, Lambrecht W R L and Segall B 1996 *Phys. Rev.* B **53** 16310
[20] Christensen N E and Gorezyca I 1994 *Phys. Rev.* B **50** 4397
[21] Wright A F and Nelson J S 1995 *Phys. Rev.* B **51** 7866
[22] Ferreira da Silva A, Souza Dantas N, de Almeida J S, Ahuja R and Persson C 2005 *J. Cryst. Growth* **281** 151
[23] Yu P Y and Cardona M 2001 *Fundamentals of Semiconductors* 3rd edn (Berlin: Springer)
[24] Kalarasse F and Bennecer B 2006 *J. Phys. Chem. Solids* at press
[25] Alouani M, Brey L and Christensen N E 1988 *Phys. Rev.* B **37** 1167
[26] Gorezyca I, Christensen N E and Alouani M 1989 *Phys. Rev.* B **39** 7705
[27] Lambrecht W R L and Rashkeev S N 2000 *Phys. Status Solidi* b **217** 599
[28] Huang M-Z and Ching W Y 1993 *Phys. Rev.* B **47** 9449
[29] Kootstra F, de Boeij P L and Snijders J G 2000 *Phys. Rev.* B **62** 7071
[30] Persson C, Ahuja R, Ferreira da Silva A and Johansson B 2001 *J. Phys.: Condens. Matter* **13** 8945